Measurement of flow field and local heat transfer distribution on a scraped heat exchanger crystalliser surface

Marcos Rodriguez, Florent Ravelet, Rene Delfos, Geert-Jan Witkamp

Measurement of flow field and local heat transfer distribution on a scraped heat exchanger crystalliser surface

M. Rodriguez Pascual[1], F. Ravelet[2,3], R. Delfos[2], G.J. Witkamp[1]
[1]Process & Energy Dept. Delft University of Technology, The Netherlands
[2]Laboratory for Aero and Hydrodynamics, Delft University of Technology, The Netherlands
[3]Laboratoire d'Energétique et de Mécanique des Fluides Interne, France

Corresponding author:

Marcos Rodriguez Pascual
M.Rodriguez@wbmt.tudelft.nl
Tph: +31-15-2786605
Fax: 0031-15-2786975

Co-authors :
René Delfos
R.Delfos@tudelft.nl
Florent Ravelet
florent.ravelet@laposte.net
Geert-Jan Witkamp
G.J.Witkamp@xs4all.nl

Abstract

In a cylindrical scraped heat exchanger crystallizer geometry the flow field influence on the local heat transfer distribution on an evenly cooled scraped heat exchanger surface has been studied by direct measurements of the heat exchanger surface temperature and the fluid velocity field inside the crystallizer.

Liquid Crystal Thermometry revealed that the local heat transfer is higher in the middle area of the scraped surface. Stereoscopic PIV measurements demonstrated that the secondary flow inside the crystallizer is responsible for this phenomenon. These local heat transfer inhomogeneities on the heat exchanger surface reduce the control over the onset of the formation of an isolating scale layer, and therefore limits the production capacity of the crystallization process.

Keywords: Heat transfer, Heat exchanger, Scraped heat exchanger crystallizers, Cooling crystallization, Scale formation, Flow field measurements, PIV, LCT,.

Nomenclature

C_p	specific heat (J/kgK)
d	hydraulic diameter (m)
h	heat transfer coefficient (W/m^{2}K)
Nu	Nusselt number (-)

p	pressure (Pa)
Pr	Prandlt number (-)
$\dot{Q}$	heat flux (W)
$\dot{q}$	surface heat flux (W/m^2)
r	radial coordinate (m)
Re	Reynolds number (-)
t	time (s)
T	temperature (K)
Vol	volume (m^3)

Greek

δ	thickness (m)
ϕ	flow rate (m^3/s)
λ	thermal conductivity (W/m K)
ρ	density (kg/m^3)
Σ	Thermal liquid + Stainless steel plate+ Vaseline + (Liquid crystal layer / 2)

Subscripts

thl	thermal liquid
feed	feed solution
HE	Heat exchanger
loss	heat loss to the surroundings
stst	stainless steel plate
lc	thermo-chromic liquid crystal underneath a polyester sheet
sol	solution

1 Introduction

Several cooling crystallization processes consist of solutions or melts that by the action of heat exchangers are brought into supersaturated regions where crystals will be formed. In industrial continuous processes, where liquid is constantly fed into the crystallizer, control and stability of the bulk solution temperature is mandatory. For this reason a degree of turbulent flow in the crystallizers is necessary to achieve good mixing of the whole solution. The heat transfer rates are

directly responsible for the production rates. The residence times of the suspension in the crystallizer will determine size and quality of the crystals.

To obtain the desired supersaturation in cooling or eutectic freeze crystallization the melt or solution is cooled down by heat exchangers (HE) that are in direct contact with the liquid. Near the HE surface a thermal boundary layer exists which a thickness that depends on the crystallizer flow characteristics. In this layer the supersaturation is higher that in the bulk solution. Because of the higher supersaturation nucleation and growth of crystals at the HE surface happen faster than in the bulk liquid. This situation is responsible for the formation of an isolating scale layer of crystals on the HE surface in cases where the temperature difference between the bulk liquid and the cooling liquid in the HE is too high. As a consequence the heat transfer decreases, which affects not only the production rate but also the stability of the crystallization process. To avoid this scale layer formation, it is common to use mechanical actions such as scraping.

The scraping efficiency that is needed to keep the HE surface clean is directly proportional to the temperature difference between the bulk solution and the HE surface temperature [1, 2]. Depending on the composition of the solution or the melt and the characteristics of the mechanical scraping action (velocity and shape of the scraper, and thus of the forces applied by the scraper), a maximum temperature difference between the liquid and the HE surface can be maintained without the appearance of scaling. The temperature across the HE surface also has to be as uniform as possible to avoid cold spots where scale formation is initiated, that subsequently spread laterally over the HE surface. Even for homogeneously cooled HE surfaces the occurrence of cold spots is often noticed. For this reason the influence of the fluid flow solution inside the crystallizer on the local heat transfer conditions at the scraped HE surface was studied here. A crystallizer with a flat bottomed cooling surface was specially designed to investigate ice scale formation from an aqueous electrolyte solution. This ice scaling crystallizer (ISC) was used before by Vaessen[1] and Pronk[2], who used this equipment to study ice scaling from various electrolyte solutions.

2 Ice scaling Experiments

2.1 Setup

The experimental set-up for the study of ice-scaling consists of a 10 liter crystallizer of 200 mm diameter and 300 mm height with a scraped HE surface at the bottom as shown in Figure 1. The 1 mm thick stainless steel bottom plate has a heat transfer area of 0.031 m^2, which is scraped by four rotating Teflon scraper blades of 99 mm driven by a vertical shaft. Halfway this shaft, a turbine mixer with a diameter of 100 mm is installed to keep the slurry well mixed. The HE plate is

cooled underneath by a 50 wt% potassium formate solution. The coolant flows at a high flow rate through a coupled inlet/outlet spiral channel below the HE plate to avoid temperature differences across the HE surface. The height and width of the channel are 5 and 17 mm respectively. The flow rate of the coolant in the channel is over 3 m/s, which guarantees turbulent channel flow. The HE inlet temperature is controlled within 0.1 K by a cooling machine.

Figure1

To study a continuous process, we have a feed flow entering the vessel at a height of 200 mm from the bottom. The crystallizer then overflows to an ice-melting vessel where the produced ice crystals are molten, and from which an aqueous solution is pumped back to the crystallizer through the feed flow, thus creating stationary flow conditions. To minimize heat leaks to the surroundings, the experimental set-up was thermally insulated wherever appropriate, apart from the few parts that were required for visual observation.

The temperatures of the coolant at the inlet and outlet, the temperature of the solution close to the top and the bottom of the crystallizer at the height of 45 and 220 mm, 15 mm inside the crystalliser from the wall, as well as the temperature of the feed flow were measured with an ASL F250 precision thermometer connected to PT-100 temperature sensors with an accuracy of ±0.01 °C. The pressure of the coolant in the channel was measured at the inlet and outlet by two Rosemount pressure transmitters with an accuracy of ± 0.001 bar. The flow rate of the feed solution and the coolant were measured by two Rosemount E-series magnetic flowmeters with an accuracy of ±1 l/h. The five temperatures, the two pressures and the two flow rates were recorded every 1 second by a computer using a data acquisition program.

2.2 Observations

During all experiments the temperature of the solution in the crystallizer was initially kept constant at the freezing temperature of the water of the salt water system. Subsequently the heat flux through the HE was gradually increased by lowering the HE temperature. During this procedure we observed that ice scaling (i.e. the formation of ice that is not removed by the scraper blades) starts in two distinct areas of the HE surface from where it spreads in all lateral directions until it covers the whole HE surface. These areas were located around the scraper shaft in the centre of the surface and close to the outside wall. When this process of scale formation continues, the scrapers are gradually lifted up from the surface, and their scraping action quickly deteriorates. In this way first two rings of hard transparent ice layers were formed at the centre and at the outside of the HE, followed by a less compacted softer not transparent ice layer in the middle area as can be seen in Figure 2.

Figure 2

In cooling experiments performed in a scaled-up version of this crystallizer, exactly the same behavior was observed [3]. In this scaled-up version the scrapers are independent modules with their own applied forces. As the cooling is continued after the first onset of scaling close to the outside wall it ends by damaging the outer part of the scraper blade, while the scraper blade close to the shaft is still capable to remove the forming ice layer (Figure 3).

Figure 3

Three different explanations for the first occurrence of scaling close to the shaft and close to the wall were investigated:

1) Inhomogeneity in the scraper function
2) Inhomogeneity in the liquid temperature above the scraper
3) Inhomogeneity in the heat flux through the thermal boundary layer.

1) The first explanation could be that the scrapers function better in the middle section of the blade. To investigate if this were true the HE surface was coated with permanent ink. Because the load force was applied by springs attached to the plastic scrapers (see figure 3) the scraping action was slightly better at the spring locations, but these locations did not match with the position in the middle of the HE surface. We nevertheless solved the problem of the unevenly applied force by the springs by applying this force through a pneumatic air pressure balloon between the holder and the scrapers. This force now imposed a uniform and controllable scraping action on the HE surface. After this improvement exactly the same ice scaling areas were observed. Also attempts to avoid differences in force applied by the scraper along the length of its blade by dividing each scraper arm in three independent scraper sections with their own spring loading did not change the observed scaling pattern. So we discarded this explanation.

2) Secondly the influence of the feed flow inlet on the scaling pattern was investigated. The feed flow inlet is always slightly warmer than the crystallizer fluid. We have visualized the flow pattern by injecting a blue dye into the feed flow. Snapshots of the experiments with a time difference of 1 second after injection of the dye are shown in Figure 4.

Figure 4

When entering the crystallizer, the dye is first transported upwards, and then mixed in the top section, before it finally descends onto the lower section where it contacts the HE surface. By that time, it is well mixed, and cooled down sufficiently to have no impact on the surface temperature of the HE. So the only possible explanation that remains is that the local heat transfer varies over the

bottom HE plate. Therefore in-situ measurements were performed to register the HE surface temperature distribution, and consequently the local heat flux distribution. In addition quantitative flow measurements were done.

3 Heat Exchanger Surface Temperature Measurements

3.1 Experimental Setup

The set-up for measuring the scraped HE surface temperature field is shown in Figure 5.

Figure 5

This temperature was measured by using an adhesive thermo chromatic liquid crystal sheet (TLC sheet), Hallcrest R34C1W, placed directly onto the HE-surface using 0.03 mm of vaseline, with thermal conductivity of 0.2 W/mK, to ensure close contact between the layers. The liquid crystal changes colour with temperature, with a working range between 34-35 °C (provider-specified). The thermo chromic liquid crystal layer of 0.03 mm is covered with a transparent polymer layer of 0.1 mm forming the TLC-sheet of 0.130 mm. This TLC-sheet is illuminated using a slide projector with 'white light' (320 W halogen lamp, colour temperature 3400 K). Its light is passed through a linear polarizing filter, then projected via a mirror onto the bottom of the tank under an angle of incidence of about 15° with the vertical direction ('lighting angle'). The TLC-sheet surface was observed from above under an angle of 15° as well ('viewing angle') through a second polarizer using a digital photo camera (Canon Powershot S2 IS). The two polarizers suppress unwanted reflections of the illuminating light, resulting in more saturated TLC-reflected colours. The photographic colour images (jpeg-compressed, 2592*1944 px) of the liquid crystal were recorded, and transferred to a PC every 2 seconds, on which further image processing was done using MatLab, v. 6.0.

Calibration of the TLC sheet colors was done in situ. During a gradual heat-up and cool-down procedure when the temperature on top of the TLC sheet and the temperature of the coolant, recorded by Pt100 sensors, were stable and had reached the same value within 0.01 ^{o}C, an image was selected for the calibration curve. The Red-Green-Blue (RGB) data was mapped to Hue-Saturation-Intensity (HSI) data using MatLab's rgb2hsv function. Based on the Hue values H, we obtained a one-to-one relationship for T vs. H. The useful part of the resulting calibration curve, as shown in Figure 6, is in the range 33.5 °C < T < 36 °C and was shown in Delfos & Lagerwaard [4] to depend only little on the illumination intensity with an accuracy of ±0.03 °C.

Figure 6

To avoid hysteresis effects of the TLC due to the working range we decided to study the HE surface temperature in an inverted experiment, where instead of cooling down of a solution from a temperature above the working range, we heated up a solution of about 32 ^{o}C. In this way exposure of the TLC sheet to high temperatures was avoided. So the solution was kept at a temperature of about 32 ^{o}C and was heated through the HE surface with a thermal liquid of 42 ^{o}C, while the feed flow was about 28 ^{o}C. Figure 7 shows the temperatures of the in and outgoing thermal liquid in the HE as well as the temperatures of the bottom, top and feed solution in the crystalliser versus time during the experimental measurement of the HE surface temperature.

Figure 7

The difference between the in and outgoing thermal liquid in the crystallizer is about 0.5 ^{o}C, and the difference between top and bottom solution in the crystalliser about 0.1 ^{o}C. After this stationary situation was obtained (monitored using thermometers), the imaging was started. In Figure 8 we see a typical picture of half of the TLC sheet on the heat exchanger as measured during the experiment.

Figure 8

The shiny part is one of the steel arms that hold the scraper. This result immediately shows that, even though at first glance the process as a whole is stationary, there is a strongly non-uniform temperature distribution on the HE surface.

3.2 Results - integral heat transfer

The total heat flow through the heat exchanger surface into the crystallizer, $\dot{Q}_{HE}$, directly follows from the integral energy balance:

$$\dot{Q}_{HE} = \left(\phi_{thl} \cdot \left(\rho_{thl} \cdot c_P \cdot \Delta T_{thl} - \Delta p\right)\right) - \dot{Q}_{loss} \qquad (1)$$

where ϕ_{thl}, ρ_{thl} and c_V are the flow rate, density and specific heat of the thermal liquid; ΔT_{thl} and Δp are the temperature and pressure drop of the thermal liquid in the channel, and $\dot{Q}_{loss}$ is the heat flux to the surroundings. The loss of heat was determined in earlier experiments for this HE [5], and is estimated to be 1.5 W/K. For the experimental conditions given above, the heat transferred into the crystallizer was 190 W. For not stationary heating as in our case, this net heat flow is absorbed by the solution and the feed:

$$\dot{Q}_{HE} = \dot{Q}_{feed} + Vol \cdot \rho_{sol} \cdot c_P \cdot dT_{cryst} / dt\,, \qquad (2)$$

where $\dot{Q}_{feed}$ is calculated in a similar way as the $\dot{Q}_{HE}$. This gives a $\dot{Q}_{feed}$ of 120 W average during the measurement time, which means a total uptake of heat by the solution of 70 W and an increase in temperature of 0.4 ^{o}C.

The dT_{cryst}/dt obtained from the measurements, equals 0.0017 ^{o}C/s and therefore the total increase in temperature during the experiment of 4 minutes is also 0.4 ^{o}C. This value matches the value as calculated from the total heat flow through the HE surface.

.

3.3 Results - local heat transfer

Above we considered the total heat transfer from the thermal liquid to the crystallizer solution. Since the HE surface temperature was observed to be much dependent on the specific location, it is more relevant to calculate the local heat flux $\vec{J}_q(r)$as a function of the radius. Because the TLC colour pattern on the HE surface is more or less axial symmetric, all profiles are assumed to be functions of only the distance to the centre, *r*. The local relationship between $\vec{J}_q(r)$ and the heat transfer coefficient $h_{\Sigma,}$ up to half of the liquid crystal layer thickness, can thus be represented by [6]:

$$\vec{J}_q(r) = h_\Sigma \cdot \left(\overline{T_{thl}} - T_{lc}(r)\right) \qquad (3)$$

where $\overline{T_{thl}}$ is the average temperature of the thermal liquid of 41.4 ^{o}C, and $T_{lc}(r)$ the local liquid crystal temperature.

The heat transfer coefficient h_Σ is calculated by summing the individual heat resistances:

$$1/h_\Sigma(r) = 1/h_{thl} + \delta_{stst}/\lambda_{stst} + \delta_{lc/2}/\lambda_{lc/2} + \delta_{Vaseline}/\lambda_{Vaseline} \qquad (4)$$

Here the thermal conductivities for the stainless steel plate and the liquid crystal are 16 W/m.K and 0.2 W/m.K, respectively. To obtain the convective heat transfer coefficients at the thermal liquid channel side, h_{thl}, is more complicated. For a flowing liquid, it is given by $h_{thl} = Nu_{thl}.\lambda_{thl}/d$, with d the hydraulic diameter of the duct, which is 7.7 mm. The Nusselt number Nu for turbulent straight duct flow is given by [6]:

$$\mathrm{Nu} = 0.024 \cdot \mathrm{Re}^{0.8} \cdot \mathrm{Pr}^{0.3} \qquad (5)$$

A result found previously for a turbulent flow in the heating channel [5], used here, was about twice as large due to the curvature of the channel which improves heat transport, so:

$$\mathrm{Nu} = 0.0507 \cdot \mathrm{Re}^{0.699} \cdot \mathrm{Pr}^{0.33} \qquad (6)$$

For our typical flow conditions, Nu = 42 hence h_{thl} = 2800 W/m^2.K.With the four now known heat resistances (h_Σ = $h_{\ thl+stst+Vaseline+lc/2}$), we can calculate the local heat flux $\vec{J}_q(r)$ between the HE thermal liquid side and the liquid crystal temperature values.

As a validation of the measured $T_{lc}(r)$, the integrated heat flux over the total HE surface was calculated to be 190 W, which matches well with the heat flow value from the total energy balance.

The temperature values $T_{lc}(r)$ were derived from the photographic image of the liquid crystal by selecting the area between scrapers (Figure 9a), and by converting the RGB values into Hue values (false colors, Figure 9b), that were then transformed into real temperatures with the calibration curve (Figure 9c).

Figure 9

As could be expected from the ice scaling observations, the heat exchanger surface temperature is far from uniform. At the measured temperature difference between thermal liquid and the solution of 10 ^{o}C, the local HE surface temperature varies by more than 4 ^{o}C. The radial profiles of the temperature distribution of the liquid crystal ($T_{lc}(r)$) and the related local heat flux $\vec{J}_q(r)$ are shown in Figure 10.

Figure 10

We now indeed clearly see that the local heat flux $\vec{J}_q(r)$, is lower near the crystallizer centre and close to the outside crystallizer wall than somewhere halfway the radius by a factor of at least five. This observation of temperature and heat transfer distribution fully explains the observation of ice scaling in the ISC experiments. In regions where the heat flux is low, the HE surface temperature drops to lower values, thereby increasing the supersaturation of the solution. Hence in these regions nucleation and growth of ice crystals will occur much faster, and thus also the tendency towards scaling. The question however, remains what causes the $\vec{J}_q(r)$ to vary so much over the HE plate. These large differences could certainly not be explained by the temperature differences between the in and out going flow of the HE because that difference is as we can see from Figure 7 less than 0.5 degrees. Besides when the temperature distribution across the HE surface was measured in the same manner for calibration the HE temperature in the absence of flow motion of the solution the temperature was uniformly distributed. For this reason the flow pattern in the crystallizer as well as the turbulence present directly above the HE plate were subsequently studied.

4 Stereoscopic PIV Flow Measurements

To reveal the cause of the widely varying local heat flux, the flow field and the turbulence distribution inside the crystallizer were investigated by Stereoscopic Particle Image Velocimetry, (3C-PIV). A general description of 3C-PIV can be found in Raffel [7] and specific details of the 3C-PIV set-up used here can be found in Ravelet [8]. This set-up is sketched in Figure 11.

Figure 11

4.1 Experimental Setup

The shaft with scraper and stirrer was taken from the original crystallizer geometry with a 200 mm internal diameter and put into a slightly larger glass cylinder with a 240 mm internal diameter, which was well aligned in the two-camera stereoscopic PIV set-up described by Ravelet [8]. With the vertical-radial laser light sheet two 2D PIV images were captured from two different cameras at different positions, which represent two different projections of the particle motion. The 3D calibration, the laser and camera timing as well as the PIV image processing were all done using Davis 7.1-7.2 (www.Lavision.de).

The measured 2D area inside the cylinder was 45 mm high and 80 mm wide, and started just above the scraper and at the outer wall, as shown in the left hand picture of Figure 11.

4.2 Results

From 500 instantaneous flow fields the average flow velocities were calculated. The instantaneous velocity field as given in Figure 12 shows that the flow is quite turbulent. For this reason a good temperature distribution inside the crystallizer is expected. To explain the variation in local heat transfer across the HE surface we have to look at the average velocity field and its impact on the local heat transfer.

Figure 12

The average flow field is shown in Figure 13a also, since the flow varies only little with height, axially averaged radial profiles can be obtained, as plotted in Figure 13b. The largest velocity component is the tangential velocity, because this velocity is dominantly imposed by the rotating scraper arms and the impeller, while the friction of the fluid with the smooth outer wall and the free surface top is small. We can therefore observe, apart from a thin under-resolved boundary layer at the outer wall, three distinct regions in the flow profile.

Figure 13 a&b

1) Up to a radius of roughly 50 mm, the tangential liquid velocity (blue) roughly matches that of the scraper-stirrer shaft (dotted red). Even though most of the data close to the shaft is failing, it only seems realistic that the whole inner region is in solid-body rotation with the scraper-stirrer shaft, with small axial and radial velocities (Figure 14).

2) Beyond 60 mm the tangential velocity decreases, and in this region the axial profile shows the existence of a strong secondary flow. Between 60 and 100 mm the fluid is flowing downwards, and near the outer wall beyond 100 mm the fluid is flowing upwards, with a magnitude of as much as

15% of the tangential velocity. This strong secondary flow component is driven by the rotating scraper arms, which near the bottom transport the fluid outwards by centrifugal force. Arriving at the outer wall, this flow is deflected upward. By continuity, the fluid has to flow somewhere else radially inwards and then downwards; here we see a maximum downward flow occurring at 80 mm from the centre. When moving radially inward or outward, the flow tends to conserve its angular momentum [9]. In a frictionless flow the result would be a potential vortex. As a simplified physical model to the flow, we fitted the measured tangential velocity profile with the Oseen vortex solution [9], which abruptly transits from a solid-body rotation inside region to a free vortex flow outside region, as shown in Figure 13b. In our case the picture matches qualitatively, but due to some mixing the transition between the two regions is more gradual than in the model.

The region of highest heat transfer is between 15 and 60 mm from the shaft, while the secondary flow comes down between 60 and 95 mm and ascends again from 100 mm. So this flow does not directly increases the heat flux in the HE surface area underneath, but it should undoubtedly play a role in the heat transfer distribution at the surface.
Therefore, we need more information about the detailed flow field in this experimentally not accessible region. This prompted us to calculate this flow field in the forthcoming paper [11].

This influence of the flow field on the local heat transfer at the HE surface and consequently on the scale layer formation may also explain some of the previous experimental results of our group (Vaessen *et al.* (2002) and Pronk[2,5]:).

- Increase of the scraping velocity, which was expected to better avoid ice formation, resulted in an earlier scale layer formation for the same solution under the same experimental conditions.
- The reproducibility of scaling experiments for the same aqueous solutions and the same temperature difference between the scraped HE surface and the solution was limited, which may be explained by small variations in local heat transfer over the HE surface, caused by the differences in the bulk flow field.

5 Conclusions

During cooling crystallization from aqueous solutions ice scaling was observed to be formed at specific areas on the HE surface. The local supersaturation is the driving force for nucleation and growth of the ice scale layer. This driving force is reflected by the difference between the HE surface and the solution temperature. The HE surface temperature was therefore measured with a liquid crystal layer, and the local heat flux through the HE was derived from it.

The local surface measurements showed that indeed the temperature on the HE surface was not uniformly distributed with temperature differences larger than 4 ^{o}C. Such differences are sufficient to explain the local variation in scaling tendency. The temperature difference directly relates to a variation in the local heat flux through the HE surface. The experimental results showed that in the middle of the scraped area the heat transfer is larger than around the shaft and close to the crystallizer wall.

A strong secondary fluid flow in this crystallizer geometry was showed by the stereoscopic PIV measurements.

This flow pattern in the crystallizer is undoubtedly related to the differences in local heat flux, but could not directly be explained without a more detailed knowledge of the flow field close to the HE surface in the scraper region.

In designing cooling crystallizers and heat exchanger geometries, it is therefore important to take flow-induced inhomogeneities in heat flux into account, since these inhomogeneities form a strong limitation in the crystallizer performance.

References

[1]Vaessen, R.J.C., Himawan, C. and Witkamp, G.J., (2002), *Scale formation of ice from electrolyte solutions on a scraped surface heat exchanger plate*. Journal of Crystal Growth, 237-239 (Pt.3), pp. 2172-77

[2]Pronk, P., Infante-Ferreira, C.A., Rodriguez Pascual, M. and Witkamp, G.J., (2005) *Maximum temperature difference without ice-scaling in scraped surface crystallizers during eutectic freeze crystallization* Proc. 16th Int. Symp. on Industrial Crystallization. pp. 1141-46

[3]Genceli, F.E., Gaertner, R. and Witkamp, G.J., (2005) *Eutectic freeze crystallization of a 2nd generation cooled disk column crystallizer for MgSO4-H2O system*. Journal of Crystal Growth , 275(1-2), pp. 1369-72.

[4]Delfos, R. and Lagerwaard, R., (2003) *Influence of large scale flow structures on convection at moderate Rayleigh numbers*, Eurotherm 74, Eindhoven, March 23-26

[5]Pronk, P. (2006) *Fluidized Bed Heat Exchangers to Prevent Fouling in Ice Slurry Systems and Industrial Crystallizers*, Ph.D.-thesis, Delft University of Technology.

[6]Mills, A.F., *Basic Heat and Mass Transfer* (2nd Edition), Prentice-Hall, 1995

[7]Raffel, M., Willert, C. and Kompenhans, J., (1998) *Particle Image Velocimetry*, Springer.

[8]Ravelet, F., Delfos, R. and Westerweel, J., (2007) *Experimental studies of liquid liquid dispersion in a turbulent shear flow*, paper 145 for TSFP-5, Munich, August 27-29

[9]Batchelor, G.K.(1967) *An Introduction to Fluid Dynamics*. Cambridge University Press.

[10]Petracci, A., Delfos, R. and Westerweel, J., (2006) *Combined PIV/LIF measurements in a Rayleigh-Bénard convection cel*". 13th Int. Symp on Appl. Laser Techniques to Fluid Mechanics, Lisbon, Portugal, June 26 – 29

[11] Rodriguez Pascual, M., Delfos, R., Ravelet, F., Derksen, J.J., Witkamp, G.J.. Large eddy simulations and stereoscopic particle image velocimetry measurements in a scraped heat exchanger crystallizer. Submitted for publication in Chemical Engineering Science.

Acknowledgments:

The authors want to thank Prof. Dr. Gerda van Rosmalen for in-depth discussions.

Figures:

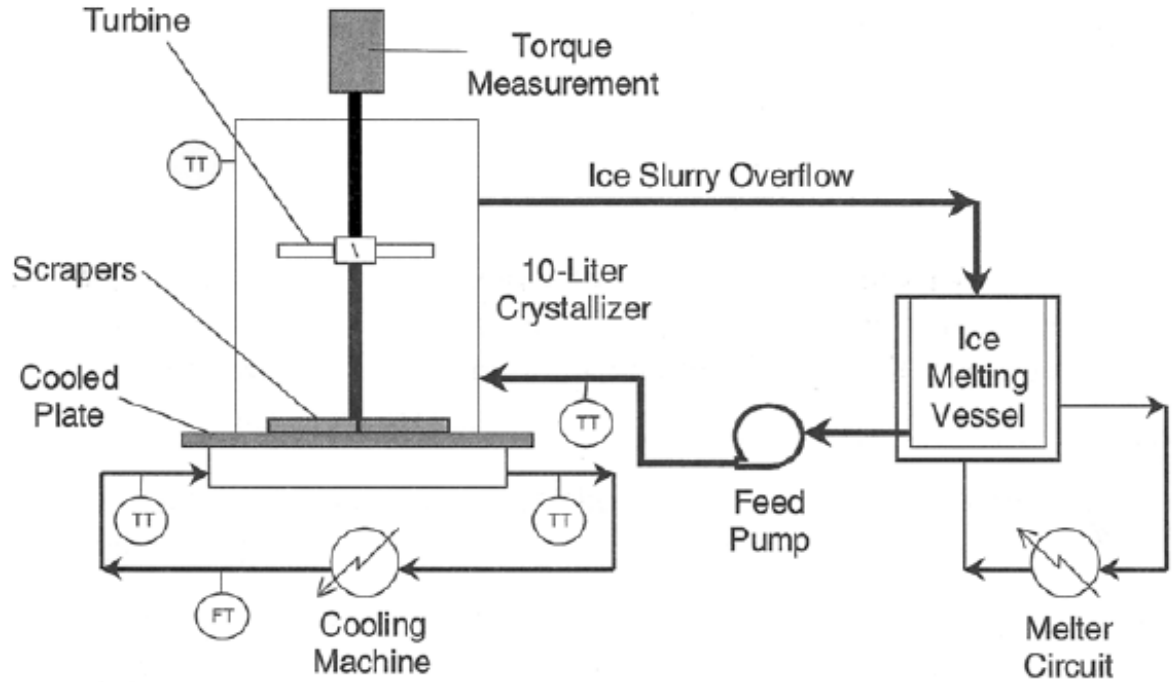

Figure 1. Flow scheme of the continuous cooling experiments.[1]

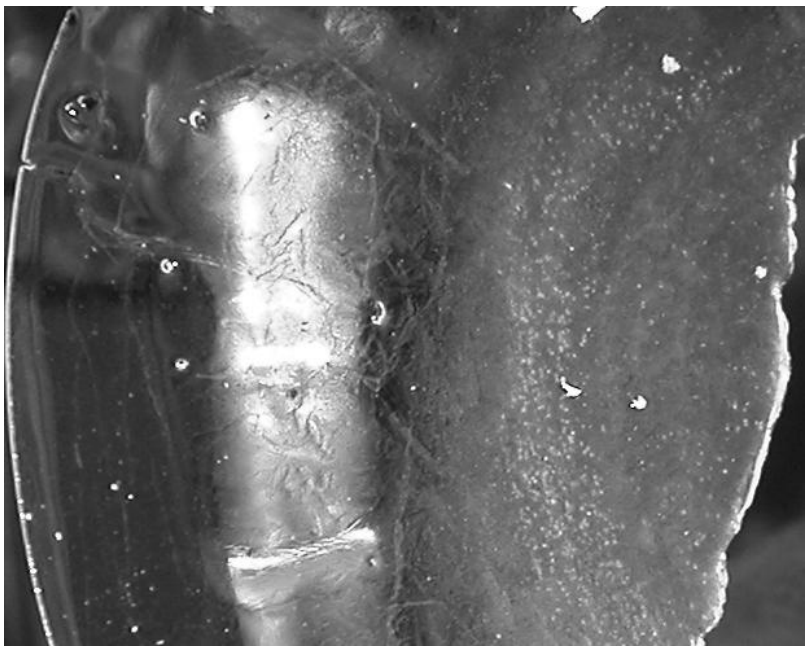

Figure 2. Ice scale layer formed on the scraped heat exchanger surface. The left transparent area corresponds to the outer area near the wall of the crystallizer. In the middle area the ice is not transparent and softer.

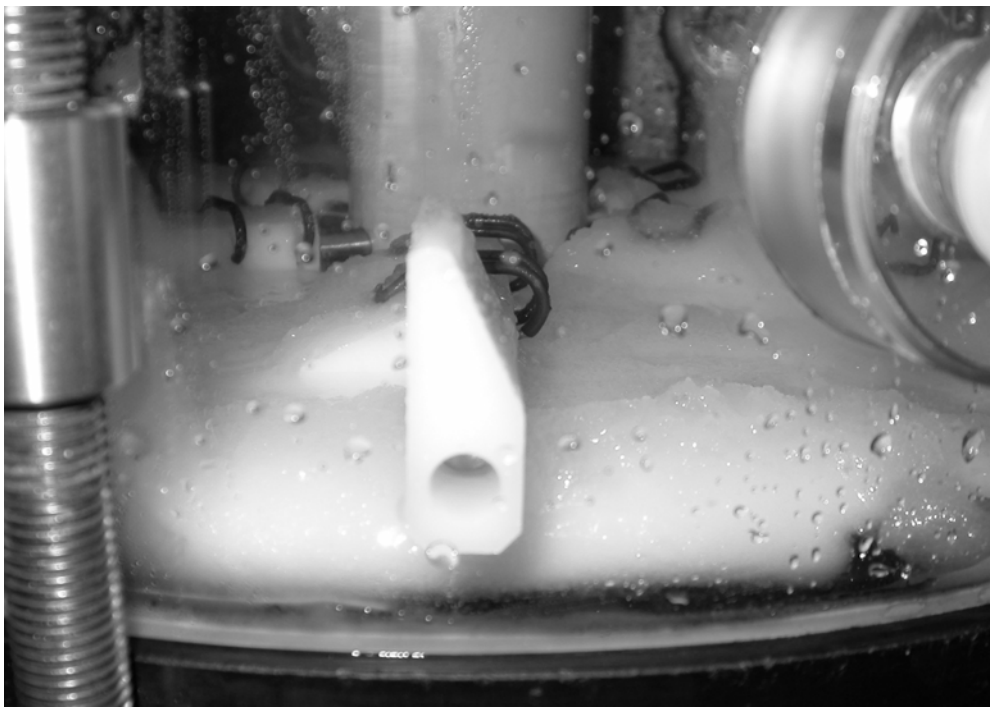

Figure 3. The same behavior as in the ISC was observed in the CDCC ending with a damaged outer scraper because of the impossibility to remove the thick ice layer formed in this area.

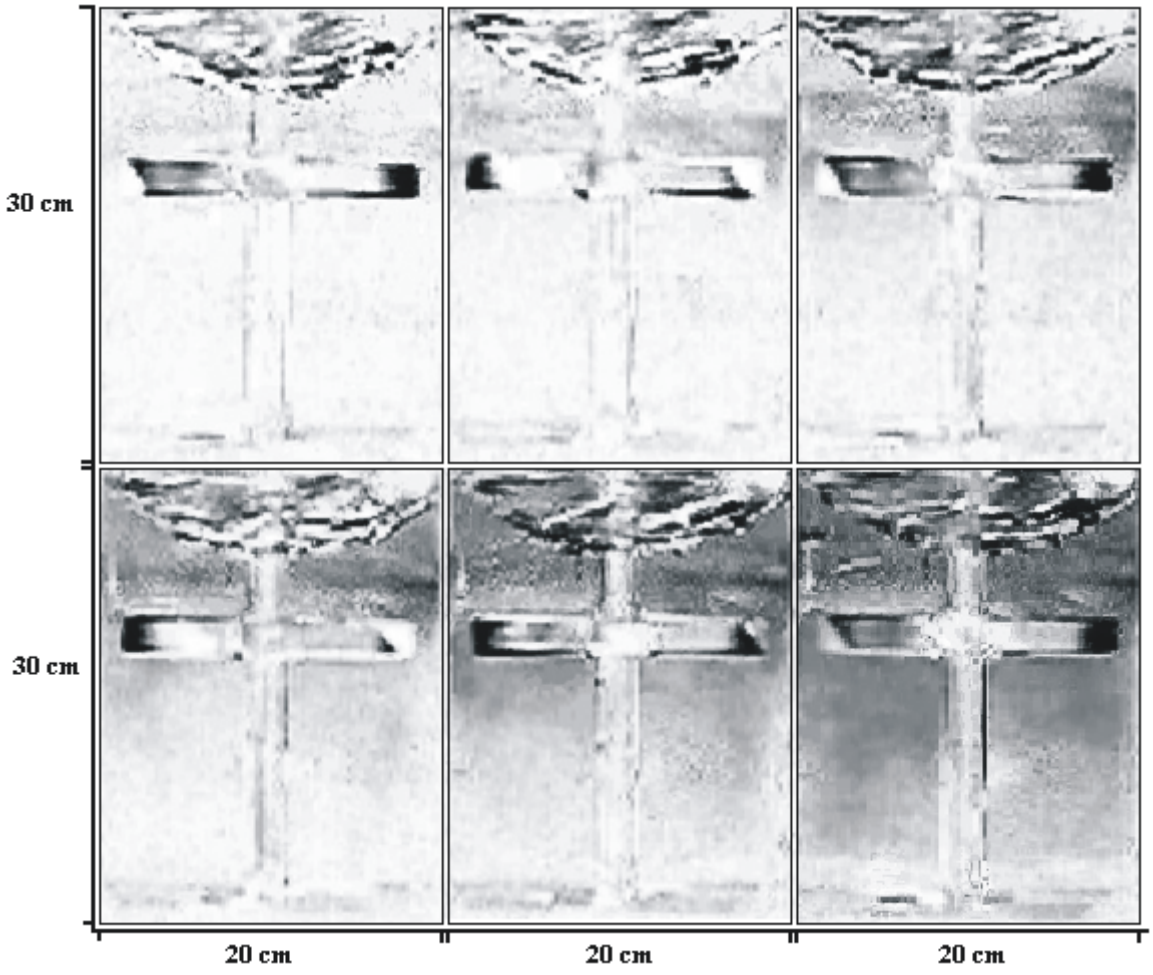

Figure 4. Snapshots of the blue dye entering with the feed flow in the crystalliser. We can see how first it is mixed in the top area and later on carried down by the impeller and mixed with the total crystalliser solution.

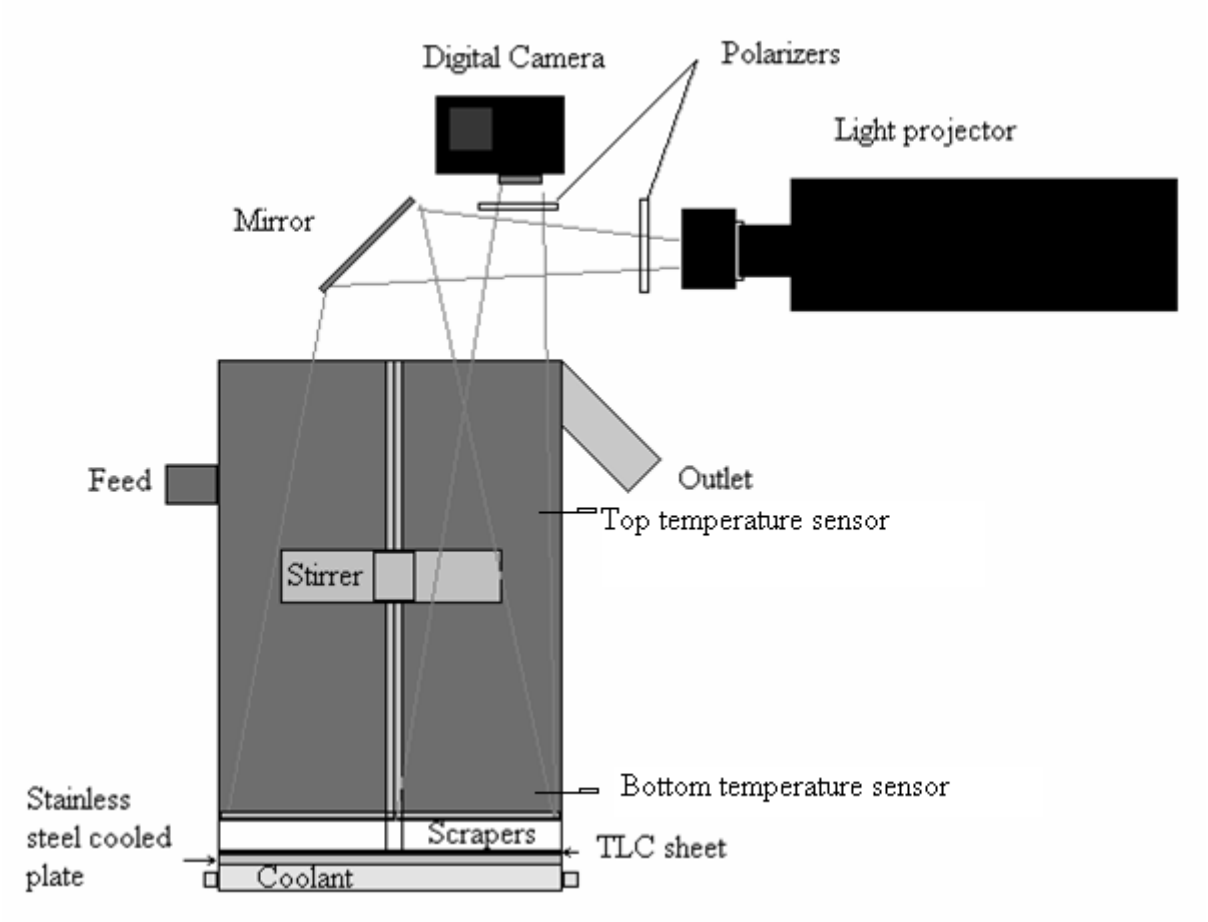

Figure 5. Sketch of the set-up for surface temperature measurement.

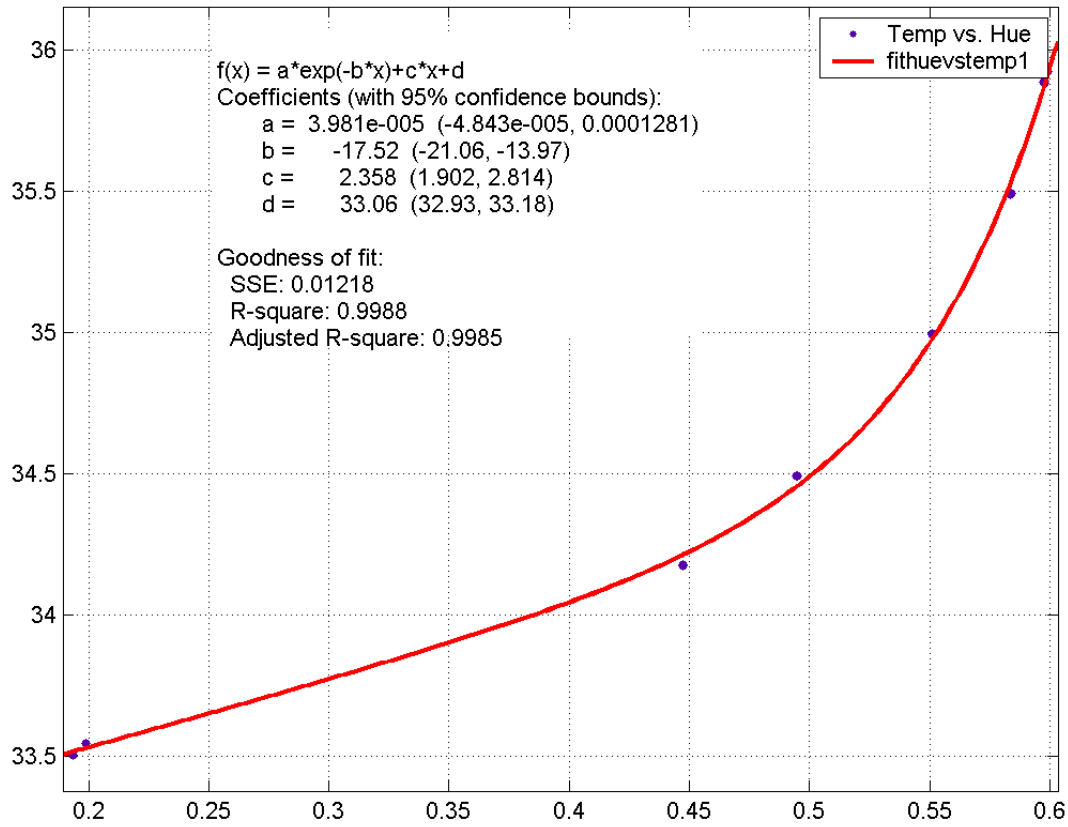

Figure 6. Calibration curve showing the direct relation between Hue and Temperature values.

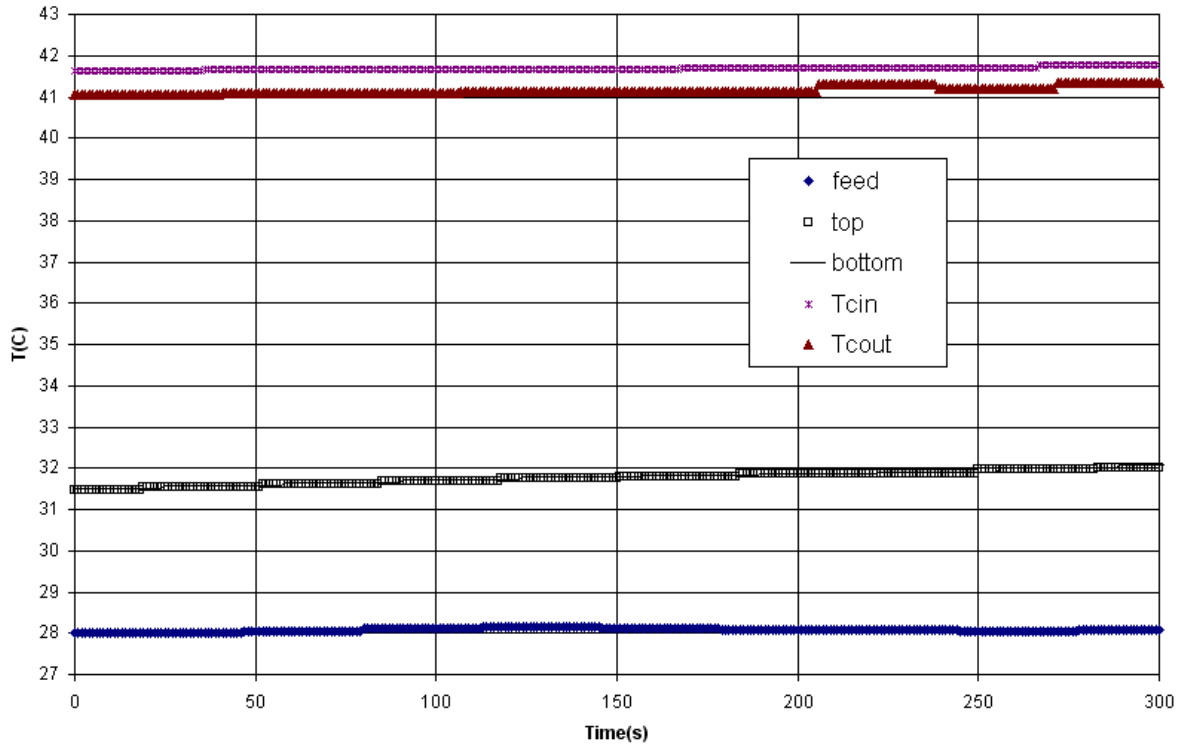

Figure 7. Temperatures of in/outgoing thermal liquid and of bottom, top and feed solution in the crystallizer during the experimental measuring period.

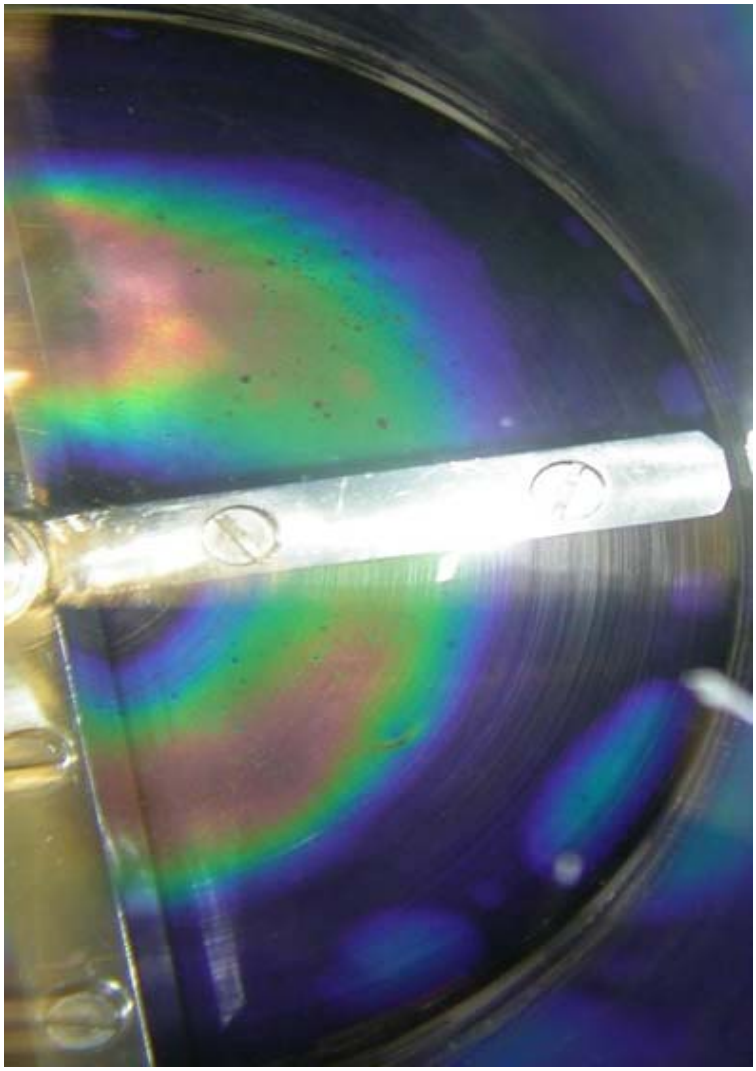

Figure 8. Image of the TLC sheet on top of the HE surface.

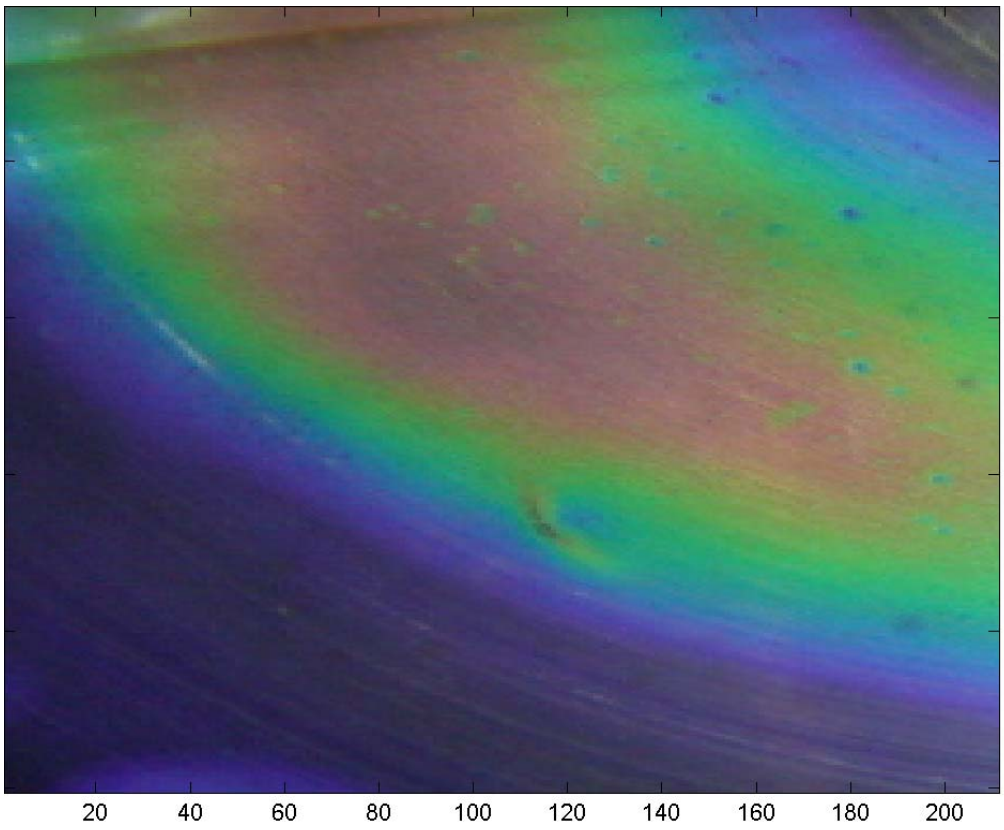

Figure 9a. Cut area in between scrapers of the HE surface.

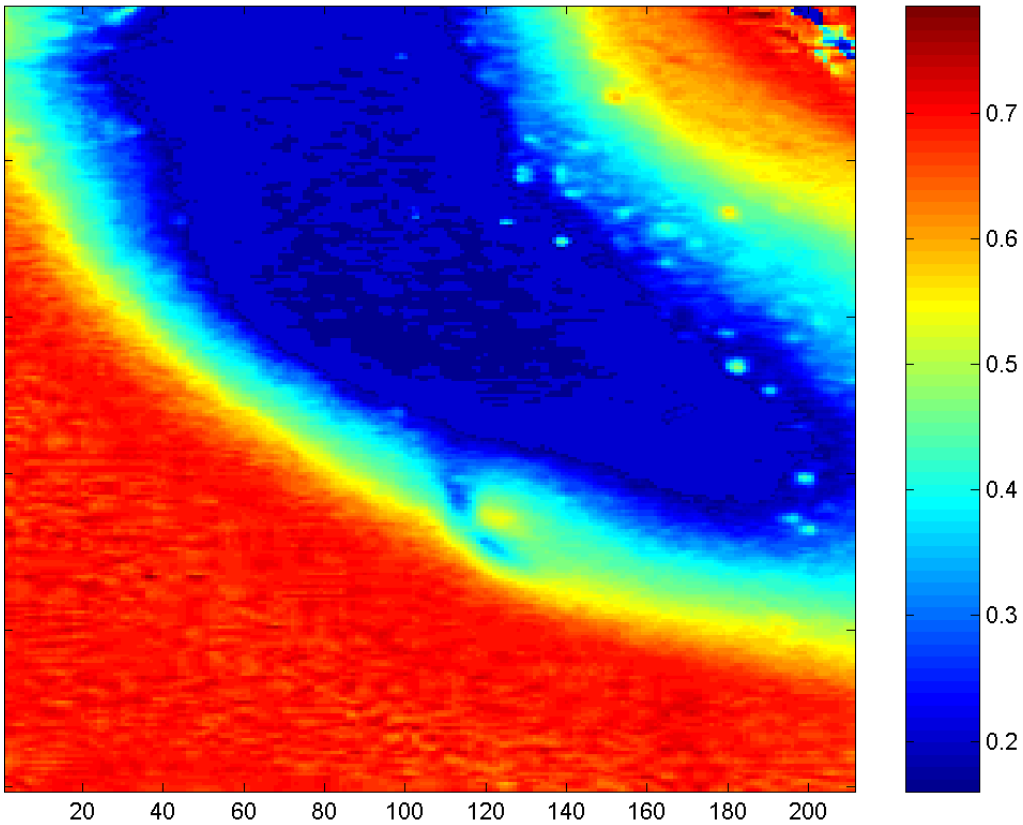

Figure 9b. Digital TLC picture converted into Hue values.

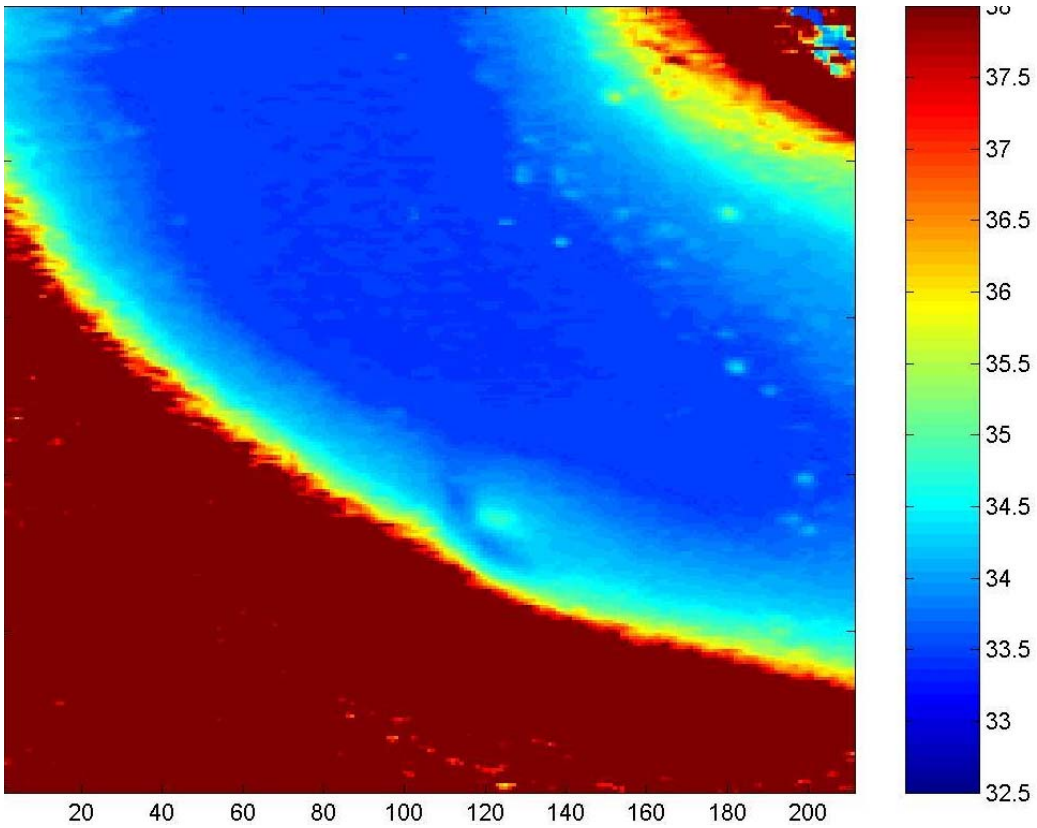

Figure 9c. Hue values converted into temperatures.

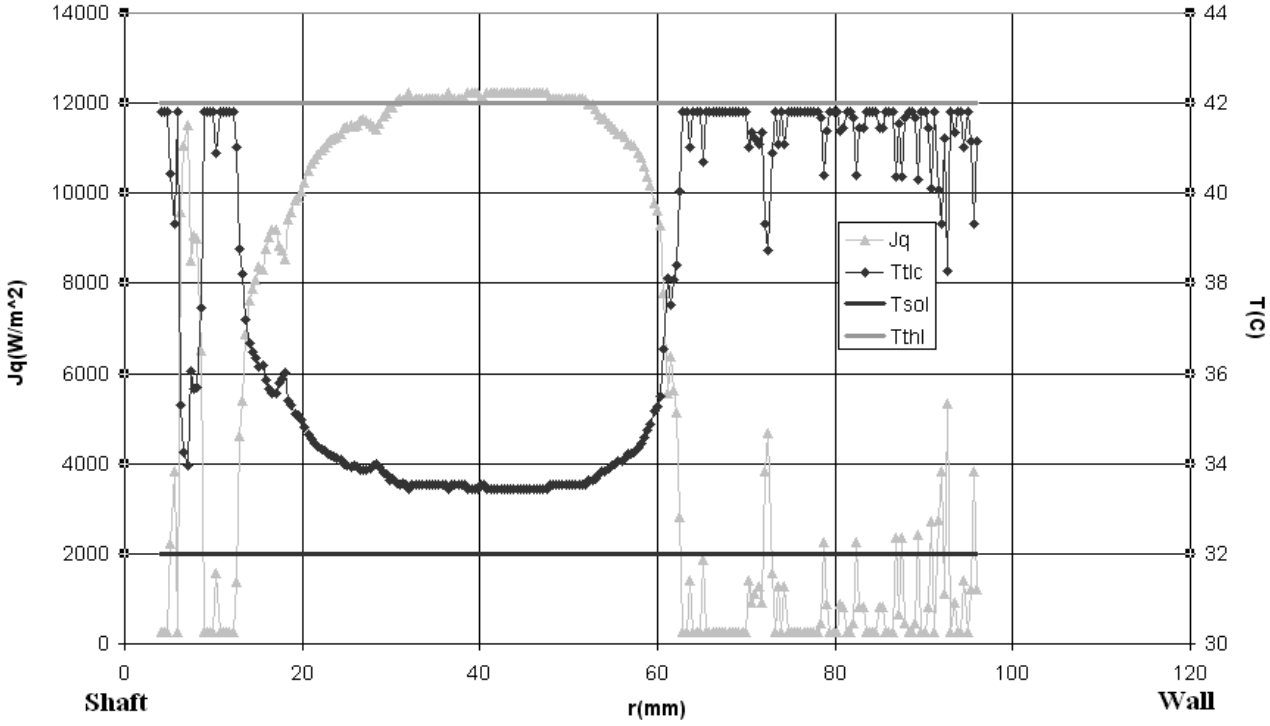

Figure 10. Radial distribution of temperature Tlc(r) and local heat flux $\vec{J}_q(r)$ (between scrapers).

Note: temperatures above 36°C are approximated (being outside the proper calibration range).

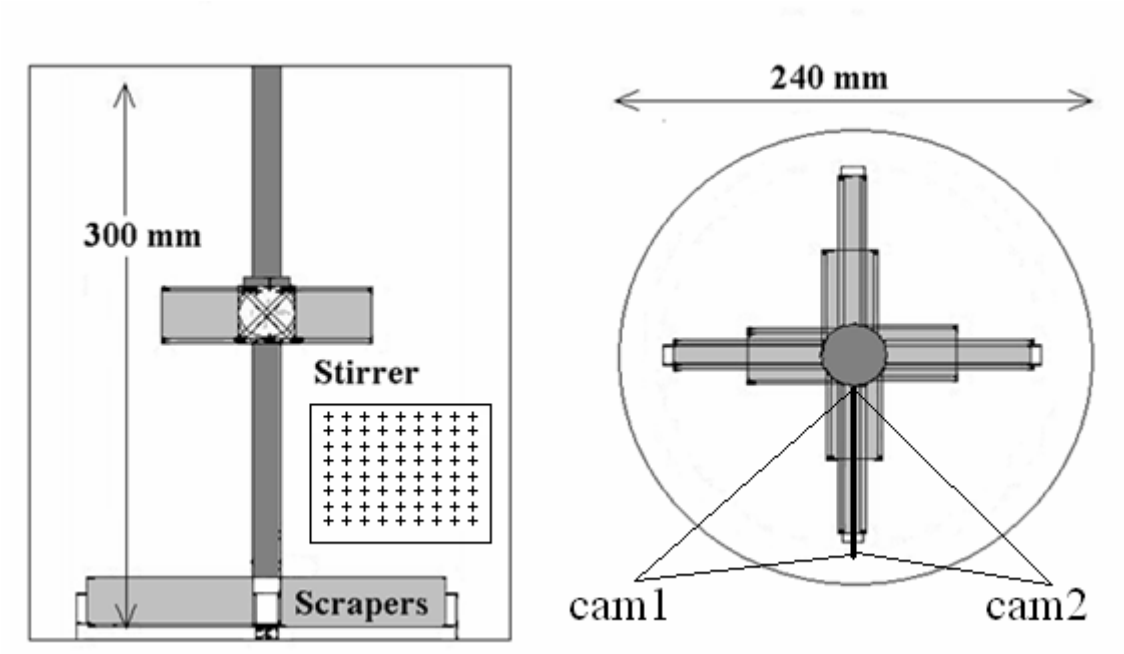

Figure 11. Sketch of set-up for PIV measurements with a PIV calibration grid-image inside.

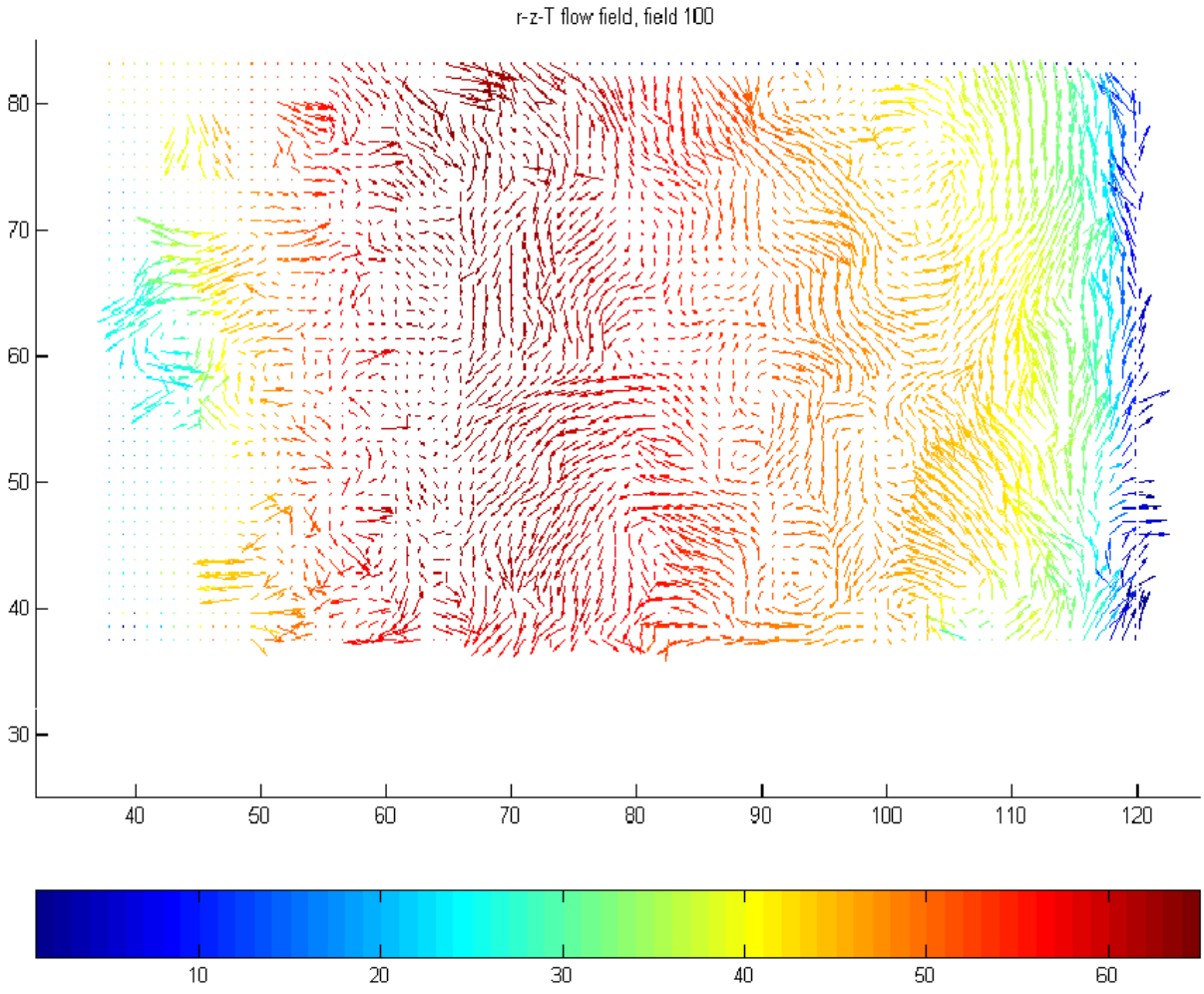

Figure 12. Instantaneous measured flow field.

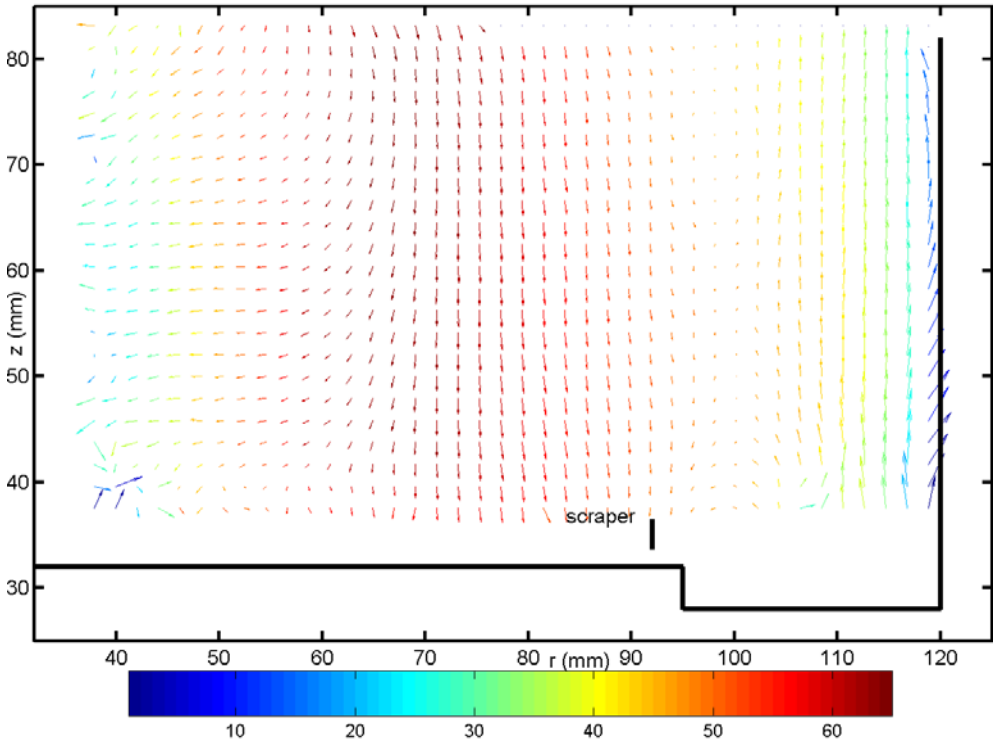

Figure 13. a) Averaged velocity field. Note: the radial and tangential components are depicted as vectors, the tangential component in false colors.

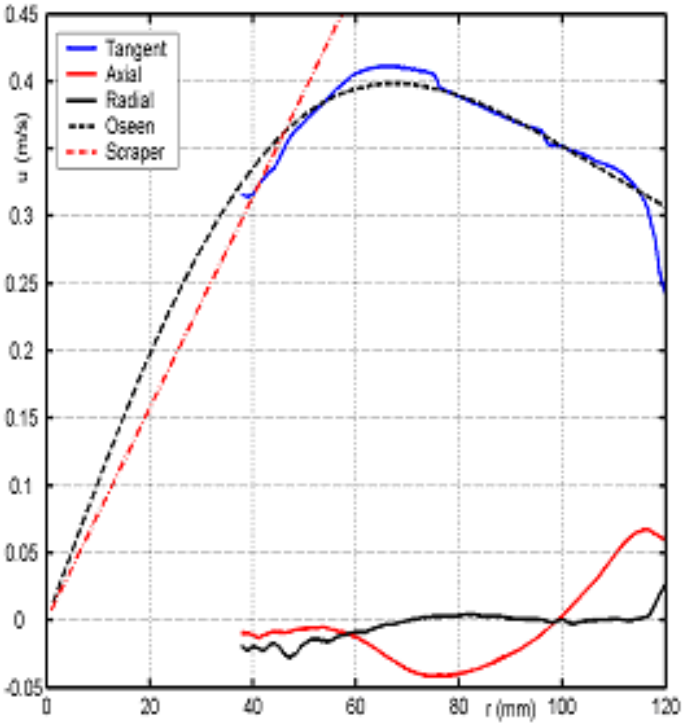

Figure 13. b) Radial profiles of velocities averaged in time and over the height of the measured PIV area in the crystallizer.